



Published in final edited form as:

Converg Sci Phys Oncol. 2016 ; 2(4): . doi:10.1088/2057-1739/2/4/045002.

Delayed Onset of Symptoms Through Feedback Interference in Chronic Cancers

Seth Haney^{1,*}, Tannishtha Reya², and Maxim Bazhenov¹

¹Department of Medicine, University of California, San Diego, La Jolla, CA

²Department of Pharmacology, University of California, San Diego, La Jolla, CA

Abstract

In many cancers, such as Chronic Myelogenous Leukemia (CML), pancreatic, and colorectal cancer, long delays exist between the initiation of the disease and the onset of debilitating symptoms. The early stages of these diseases present manageable symptoms and, in the case of CML, highly effective treatment options. Progression to the more aggressive stages of the diseases limits effective treatment and significantly exacerbates patient prognosis. The mechanisms causing delay and disease progression are largely unknown. The later stages of these diseases are characterized by excessive build up of primitive cell types, indicating a disruption in the normal cell differentiation process that is commonly regulated through feedback from differentiated types. In this study, we propose a mechanism where mutated primitive cells produce a feedback interference signal that desensitizes them to a normal homeostatic feedback. Using a mathematical model, we show that this mechanism can account for the long delay period between occurrence of genetic changes and symptomatic onset characterized by fast growth of cancerous cell population. Finally, we explore novel concepts for potential treatment of chronic cancers.

Introduction

Chronic cancers, such as Chronic Myelogenous Leukemia, CML, [1], pancreatic cancer [2], and colorectal cancer [3], are characterized by long time periods when patients remain largely asymptomatic followed by a sudden shift to the onset of aggressive and lethal disease. The early phase of many such diseases, collectively referred to here as chronic phase, allow for many effective treatment options that are less effective or impossible during the later phase, collectively referred to here as crisis phase. The time spent in the chronic phase can be long but highly variable. In particular, CML presents in multiple different phases where extreme symptoms can manifest 7–10 years after initial diagnosis [1].

What causes transitions between these different phases? Potentially, transitions happen when new genetic mutations are acquired and the length of each phase is dependent on the waiting time for new genetic hits. This would, however, imply that genetic profiling should predict the phase of the disease which may not always be the case [4]. The mechanistic origin of transitions between disease phases is therapeutically relevant. If the early phases of chronic

* Author for correspondence: *SH*, sethdhaney@gmail.com.

cancers are largely asymptomatic, then delaying progression to the aggressive phases is a very effective treatment strategy. Indeed, in the case of CML, Tyrosine Kinase Inhibitors (TKIs), do not cure CML but do prevent the progression from chronic phase to crisis phase and allow most patients to live normal lives [5].

Progression of cancer is not only marked by accumulated genetic changes. Like healthy cells, the physical [6] and biochemical [7] microenvironment is critical in determining cancer cell fate and function. Tumors modify their local microenvironment to achieve this goal by altering the extracellular signaling environment, the secretome [7]. Glioblastoma-multiformae tumors secrete angiogenesis factors [8], pancreatic cancer tumors secrete factors that increase the self renewal capacity [9], and colon cancer tumors secrete factors that preserve the tumor in an undifferentiated state [10]. These changes to the microenvironment impart their own timescales of cancer progression, independent of novel genetic mutations, and may influence the time of transition between chronic and critical phases.

Many chronic cancers develop from mutations originating in stem cells, such as CML [11], or cancer stem cells, such as colon cancer [12]. The progression of these cancers is marked by the expansion of an abnormal and non-differentiated cell population, indicating a disruption in normal control of cell differentiation processes. In healthy cell populations, the cell differentiation processes are mediated by various feedback systems [13]. These feedbacks can arise via the production of proliferative or pro-differentiative factors secreted by differentiated cell types [14–17]. In particular disruptions in the Wnt pathway (an autocrine signaling pathway) have been implicated in the onset of cancer in CML [18] and colorectal cancer [19]. Disruptions in feedback lead to disruptions in the differentiation program and can result in an overgrowth of undifferentiated cells. Deficiencies of the feedback processes that normally provide stem cell-like regulation may be a primary triggering factor in development of pathology. Indeed, previous theoretical work has identified feedback escape as a critical event in cancer initiation [20].

In this new study, we propose a model of cancer progression that depends on the feedback disruption. Feedback interference signal produced by a small population of cancerous stem cells disrupts the normal control of cell differentiation processes, leading to biphasic behavior. Initially, cancerous populations are kept low (similar to the chronic phase), but after a significant delay the cancerous population dominates the healthy population of cells (similar to the crisis phase). By exploiting dynamics of the mathematical model, we estimated the time delay to the crisis phase. We explored inter-patient heterogeneity using a stochastic model of cancer progression. Our study predicts new designs for cancer treatment that may potentially outperform conventional approaches.

Methods

To model the dynamics of cancer initiation in stem cell systems, we construct two interacting models representing normal and pathological pathways.

Model of the Normal Cell Population

In healthy cell populations, Stem Cells (SCs) differentiate to Differentiated Cells (DCs) which eventually die. The DCs produce feedback that regulates the division profile (frequency of different division types) of SCs (Fig 1A). These feedbacks ensure the homeostatic stability of cell types, see below and [20]. The Ordinary Differential Equations (ODEs) used to model this scenario are given below.

$$\begin{aligned}\frac{dSC}{dt} &= (p(DC) - q(DC))v(DC)SC \\ \frac{dSC}{dt} &= (1 + q(DC) - p(DC))v(DC)SC - dDC\end{aligned}\quad (1)$$

Here the terms p and q are the proportion of divisions representing symmetric proliferation ($SC \rightarrow SC+SC$) and symmetric differentiation ($SC \rightarrow DC+DC$), respectively. Asymmetric division ($SC \rightarrow SC+DC$) occurs with probability $1-p(DC)-q(DC)$. The overall rate of division is given by v and death rate of DCs is given by d . Here, p , q , and v are under control of feedback from DCs and hence their value depends on the DC population size.

The model we propose here is simplified to two cell types, SCs and DCs, to allow rigorous analysis. Real stem cell systems can involve multiple intermediate cell types (including an intermediate transit amplifying cells) [21] or involve a highly interconnected regulatory network of many different cell types (e.g. hematopoiesis) [22]. Since little is known about the particular feedback functions in the real biological system, we used here a Hill-like description commonly used in literature [14,20,23]. However, our main results are qualitatively the same for many different types of feedback functions (see Supplement).

$$\begin{aligned}p(DC) &= \frac{p_0}{1 + \left(\frac{DC}{\gamma_p}\right)^{n_p}} \\ q(DC) &= \frac{q_0}{1 + \left(\frac{DC}{\gamma_q}\right)^{n_q}} \\ v(DC) &= \frac{v_0}{1 + \left(\frac{DC}{\gamma_v}\right)^{n_v}}\end{aligned}\quad (2)$$

For example, symmetric proliferation proceeds at a percapita rate of p_0 in the absence of DCs. This rate decreases as the population of DCs increases, reaching 50% of its maximal value at the threshold value of γ_p and completely shutdown symmetric proliferation only for an infinite amount of DCs.

Model of Cancer Stem Cells and Feedback Interference

In cancerous cell populations, Cancer Stem Cells (CSCs) proliferate and differentiate to Cancerous Differentiated Cells (CDCs), however, CDCs, do not die in our model. This lack of death of CDCs mimics the diminishment of apoptosis in cancer. However, it should be noted that our main results do not depend on this assumption and stand when we introduced CDC death (see Supplement). The division profile of CSCs is still regulated by feedback from DCs, as in the normal pathway. The CSCs, however, produce a feedback interference signal (FI) that disrupts the feedback from DCs to CSCs in a concentration dependent manner (Fig 1B). In our model this feedback interference signal represents simplified description of a combination of intra- and extracellular signaling pathways involved in feedback regulation of the CSC division profile, a thorough discussion of the potential identity of the interference signal in biological systems is given in the Discussion. We incorporate this in the model by allowing FI to alter probability of symmetric proliferation, $p(DC)$, but not symmetric differentiation, $q(DC)$. This was in accordance with the observation that unregulated growth in many cancers is due to the aberrant self-proliferation [9,24]. In particular, we add to the ODEs above the following equations:

$$\begin{aligned}
 \frac{dCSC}{dt} &= (\bar{p}(DC, FI) - q(DC))v(DC)CSC \\
 \frac{dCDC}{dt} &= (1 + q(DC) - \bar{p}(DC, FI))v(DC)CSC \\
 \frac{dFI}{dt} &= \alpha CSC - \beta FI
 \end{aligned} \tag{3}$$

$$\bar{p}(DC, FI) \rightarrow \frac{P_0}{1 + \left(\frac{DC}{\gamma_p}\right)^{n_p} \left(\frac{1}{1 + \left(\frac{FI}{\gamma_{cm}}\right)^{n_{cm}}}\right)}$$

In this case, $CSCs$ promotes FI increase which, in turn, can disinhibit the feedback from $DC \rightarrow CSC$. If $FI \rightarrow \infty$ the $DC \rightarrow CSC$ feedback is completely shutdown. Zero FI would correspond to a fully intact feedback. The two critical parameters of this feedback are the Hill EC50, γ_{cm} , and the Hill exponent, n_{cm} , which roughly define the threshold and sensitivity, respectively, of feedback interference. We also find that alternative functional forms of feedback produce similar results (see Supplement).

In addition to the assumption that CSCs produce feedback interference (the defining property of a CSC), we make several assumptions to formulate the model of the cancerous population: 1) $CDCs$ do not die; 2) $CDCs$ do not produce feedback signal; and 3) FI only affects the cancerous population. The main finding of this work, that feedback interference causes a delay in the onset of symptoms, is not affected by relaxing any of these assumptions. For a detailed description of these assumptions see Supplement.

Calculation of Time to Crisis Phase

In this study we are primarily concerned with the time to crisis phase, where the dynamics of cancer system suddenly shift from very slow to very fast growth. We define the precise time to crisis phase by measuring when the *CSC* count crosses a threshold value, $\theta = 100 \frac{\beta \gamma_{cm}}{\alpha}$.

This amounts to 100 times the natural scaling of the *CSC* count (see Supplement).

Simulation of the Stochastic Version of the Model

We used the Gillespie Exact Stochastic Simulation Algorithm (ESSA) [25] to simulate the stochastic version of our model. Here, the model was divided into discrete events (e.g. symmetric renewal of healthy stem cells; see Table 1). The calculation of the state of the system at a future time was designed as a four step process [25,26].

1. Each event (indexed here by i) was assigned a probability of occurring, a_i , based on the rate equations (1–3). So the actual probability that event i occurs in the next small increment of time, τ , is τa_i .
2. The time to the next event of any type was then calculated as a Poisson process. Thus, inter-event times are exponentially distributed with parameter $\lambda = \sum_i a_i$. Drawing a random number from this distribution we obtain the time increment t .
3. A final random number was drawn to determine which event occurred. Here, each event occupies a proportion equal to a_i/λ of the unit interval.
4. The selected reaction was executed, the cell counts are updated, and time is incremented by t .

We use the terminology - stochastic version and deterministic version of the same model - because the function that determines the propensity (in the stochastic case) or rate (in the deterministic case) is precisely the same. Each version of the model is simulated numerically by updating the current state of the system determined by the rate (in the deterministic version) or propensity (in the stochastic version), both of which are defined by the right hand side of the equations (1–3).

Implementation of Treatment Strategies

Treatment strategies were implemented by making time-dependent alterations to the model parameters. This was achieved by multiplying these parameters by $Tr(k,t)$, where k denotes the strength and t is time. Specifics for each treatment type are given below.

Chemotherapy—A *CDC* death event is added with propensity

$$CDC \cdot Tr(k,t) = k \cdot d \cdot CDC \left(H(t) - H(t - t_f) \right).$$

Here, $k = 20$, d is the death rate of the *DC* from the normal population, $H(t)$ is the Heaviside step function, and t_f is the time that treatment terminates.

CSC-Targetted therapy—The symmetric proliferation function for the cancerous population is altered

$$\bar{p}(DC, FI) = \frac{p_0^{fTr(k,t)}}{\left(1 + \left(\frac{DC}{\gamma_p}\right)^{n_p} \frac{1}{1 + \left(\frac{FI}{\gamma_{cm}}\right)^{n_{cm}}}\right)} = \frac{p_0^{f(k \cdot (H(t) - H(t-t_f)))}}{\left(1 + \left(\frac{DC}{\gamma_p}\right)^{n_p} \frac{1}{1 + \left(\frac{FI}{\gamma_{cm}}\right)^{n_{cm}}}\right)}$$

Again $k=20$.

FI-Targetted therapy—The propensity for *FI* death becomes

$$Tr(k,t)\beta_{FI} = k \cdot (H(t) - H(t-t_f)).$$

Here $k=200$, however it should be noted that all units of treatment strength are different and, thus, not comparable.

Results

Many chronic cancers, such as CML, pancreatic, and colorectal cancer show long periods between the initial genetic onset of the disease and the onset of debilitating symptoms. This long delay, which is largely asymptomatic, is then followed by a sharp transition to symptomatic and potentially deadly phase of the disease. Because the initial phases of the diseases are largely asymptomatic they can go undetected until later phases, thus limiting treatment options. To describe a potential mechanism accounting for a delay between disease onset and symptomatic onset, we propose mathematical model of normal and cancer stem cells dynamics.

We modeled healthy populations of Stem Cells (SCs) and Differentiated Cells (DCs) by allowing SCs to undergo three different types of cell divisions: symmetric proliferation ($SC \rightarrow SC + SC$), symmetric differentiation ($SC \rightarrow DC + DC$), and asymmetric division ($SC \rightarrow SC + DC$) (see eqn. (1) in Materials and Methods). The DCs, but not the SCs, die at a constant rate. Importantly, in our model, the DCs produce a feedback signal which then can alter the relative rates, or probability, of each division type of the SCs and the absolute division rate of any type of SC division (see Fig 1). Thus, increasing size of DC population decreased rate of symmetric proliferation ($SC \rightarrow SC+SC$) and symmetric differentiation ($SC \rightarrow DC+DC$), as well as the overall rate of division (see eqn. (2) in Materials and Methods). Below, we first show that the feedback inhibitory signal can guarantee a stable dynamics with the size of all cell populations remaining constant in the normal (cancer free) conditions.

Feedbacks Ensure Stable Equilibrium in Normal Populations

Healthy SCs in vivo are responsible for maintaining a stable population of SCs, progenitors (not modeled here), and DCs. In vivo, stem cell networks are surprisingly capable of responding to drastic perturbations (for example loss of DCs) by regenerating the population to its normal level. In some stem cell systems, for example the olfactory epithelium [16], this control is mediated by feedback signals, as we have modeled here.

In the model describing dynamics of the normal cell populations in the absence of cancer, see eqns. (1,2), both SC and DC populations reach stable equilibrium (Fig 1B). Figure 1 shows dynamics over time of SC (Fig 1C) and DC (Fig 1D) populations for different initial conditions - different size of SCs and DCs populations at the beginning of simulation. In all cases the systems reached the equilibrium after a period of damping oscillations, indicating that equilibrium state was a stable focus of the dynamics system (Fig 1B–E). This type of dynamics can be explained by the negative feedback mediated by DC population [20]. Indeed, any increase in DC population led to suppression (see Materials and Methods), due to negative feedback, of both symmetric proliferation and symmetric differentiation [1] and return of the populations size to the equilibrium. Further, we found that equilibrium was achieved by the balance of symmetric proliferation ($SC \rightarrow SC + SC$) and symmetric differentiation ($SC \rightarrow DC + DC$), as one would expect (see Fig 1E). The exact size of the DC and SC populations at the equilibrium depended on the model parameters, this was reviewed in a similar model [20]. We concluded that our simplistic SC model recapitulates the robust stabilizing properties shown in normal stem cell systems.

Feedback Interference in Cancerous Populations

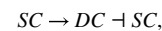
Causes Crisis Initiation After Delay—Many chronic cancers undergo long delays between genetic and symptomatic onset [1–3]. One hypothesis that can account for this delay is that symptomatic onset is determined by secondary mutations. It is known that many such cancers require more than one mutation to become aggressive and symptomatic. What is unknown, however, is when secondary mutations occur, in CML and other chronic cancers, relative to the onset symptoms. One possibility is that secondary mutations occur long before debilitating symptoms occur. In fact, CML also presents with an intermediate phase between chronic and crisis phases, called accelerated phase, which can last up to 1.5 years. This accelerated phase shows similar genetic expression to crisis phase but is symptomatically distinct.

Here we propose a dynamic mechanism via feedback interference to explain a delay between the last genetic mutation and symptomatic onset. We modeled the dynamics of the Cancer Stem Cells (CSC) population to be nearly identical to SCs, implementing the hypothesis that a small set of genetic mutations can turn SCs into CSCs and defining SCs as the cell of origin. The distinguishing feature of the CSC population is that CSCs produce a Feedback Inhibitor (*FI*), that disrupts negative feedback from DCs to CSCs in a concentration dependent manner (Fig 2A). This feedback interference signal represents simplified mathematical description of a combination of intra- and extracellular signaling pathways involved in feedback regulation of the CSC division profile (see Discussion). The CSCs also differentiate into Cancerous Differentiated Cells (CDCs), which are distinct from

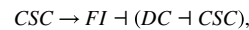
DCs in that they do not produce feedback signals and they do not undergo death (although neither of these assumptions were actually necessary for the main results presented, see Supplement).

To investigate effect of the feedback interference, we first let the model describing the normal cell population to reach equilibrium (see previous section) and we then introduced the CSC population modeled by eqn. (2) (see Materials and Methods and Fig 2A). The CSC population produced the *FI* signal disrupting normal feedback regulation from DCs to CSCs effectively leading to increase in CSC proliferation rate. The cancerous cell population grew slowly (subexponentially) until the feedback interference reached a critical amount sufficient to partially shut down the feedback mechanism (Fig 2B,C). Then, the populations underwent a strong and sudden shift to exponential growth. This sudden shift in population growth coincided with a break in the balance between symmetric proliferation and symmetric differentiation and a dominance of symmetric proliferation (Fig 2D). Furthermore, we found this transition to be robust to parameter changes, as it is shown analytically below.

Conceptually, the feedback interference changes the regulation network in the cancerous population. In normal conditions the size of the healthy population was controlled through a negative feedback loop from the *DCs*,



which gives stable *SC* and *DC* counts (Fig 1B). Feedback interference changed this control to a positive feedback in the cancerous population,



which produced unstable dynamics and unlimited growth. Positive feedback is common in biological systems and is characterized by bimodal responses [27], ultrasensitivity [28], delay to onset [29,30]. The positive feedback structure in our model was responsible for the transition to the crisis phase. However, the nonlinearities in the feedback inhibition, see eqn. (3), require critical levels of *FI* must build up before the system transitions from a minimally active (slow subexponential *CDC* and *CSC* growth) to a maximally active (exponential growth) state. Specifically, at cancer onset, low *CSC* counts implies that low, but positive, amounts of *FI* is present, thus feedback from *DC* to *CSC* remains largely intact, but less effective compared to the normal (healthy) conditions (as described in the previous section). This leads to the *CSC* population growth, but at minimal rate. As time progresses, small amounts of *FI* slowly buildup and release the *CSCs* from feedback due to *DCs*. Once this *FI* population is significantly above the threshold level, γ_{cm} , the *CSCs* undergo the transition to crisis phase. In terms of dynamical systems, because the equilibrium point is neutrally stable in the model, the system stays in the vicinity of the equilibrium until the nonlinear terms build up enough to drive the transition away from the equilibrium. Two main parameters controlled the effectiveness of the feedback interference: the threshold level or EC50, γ_{cm} , and the sensitivity or Hill exponent, n_{cm} . If the threshold level, γ_{cm} , is high it will take a larger pool of *FI* to effectively shut down the feedback inhibition. If the sensitivity, n_{cm} , is high, an amount of *FI* slightly less than γ_{cm} will have little effect on feedback inhibition, but

an amount slightly greater than γ_{cm} will completely shut down the feedback inhibition. We will frequently refer to these two critical parameters in the text below.

Stability analysis of this system revealed a large time scale separation between fast variables describing *FI* dynamics, and a slow variable describing *CSC* dynamics. Under the appropriate conditions (see Supplement), we were able to exploit the time scale separation using a center subspace approach to derive an analytical expression for the time from the cancer initiation (characterized by the last known genetic mutation) to the crisis phase, T_{crisis} .

$$T_{crisis} \approx \left(\frac{\gamma_{cm}\beta}{\alpha \cdot CSC_0} \right)^{n_{cm}} \frac{1 + (DC_{\infty}/\gamma_p)^{n_p}}{n_m p_{\infty} v_{\infty} (DC_{\infty}/\gamma_p)^{n_p}} \quad (4)$$

Here, infinity subscripts denote steady state values of DC , $p(DC)$ and $q(DC)$ (see Supplement). This approximation of T_{crisis} is dependent on the assumption that the initial amount of CSCs, and therefore initial feedback interference is close to zero. Specifically we require that $\frac{\alpha CSC_0}{\beta \gamma_{cm}} \ll 1$ (see Supplement). The time to crisis phase was primarily influenced by the initial *CSC* count, CSC_0 multiplied by the number of *FI* molecules produced by each *CSC* at steady state, α/β , relative to the threshold for feedback interference, γ_{cm} . Further, time to crisis grew polynomially with the inverse of this ratio raised to the Hill exponent of feedback interference, n_{cm} (Fig 2D). To summarize, the model predicts that time to crisis can be increased (leading to a longer delay of the problematic symptom onset) by decreasing the initial *CSC* count (Fig 2E), decreasing the influence of *CSCs* on *FI*, or increasing the threshold for feedback interference.

Our feedback interference model predicts a dynamical mechanism governing the delays and transitions between asymptomatic and aggressive phases of the chronic cancers. This idea is different from a model where another mutation is necessary to trigger the aggressive phase. In our model, the mutation that gives rise to the production of a feedback interference signal effectively switches the regulation of *CSCs* from a negative feedback, which is responsible for the control of the population in healthy SCs, to a positive feedback, which produces both delays and eventual explosive growth. This drastic shift in the control structure can account for both the delays and the sharp aggressive onset seen in the intermediate phases of chronic cancers. While this model does not exclude possibility of other mutations, it does not require them to explain the long delays seen between phases in many chronic cancers. Below, we compare our dynamic, feedback interference mechanism to canonical genetic deletion models in their ability to describe this delay and sharp transition.

Genetic Deletion of Feedback Receptor Causes Immediate Growth of Cancer Population

Loss of feedback inhibition can explain progression to more aggressive phases in chronic cancers. In our model, this mechanism is triggered by specific “mutation” that allows *CSCs* to produce a feedback interference signal. This feedback interference mechanism is responsible for long delays and sudden shifts without subsequent genetic mutation events. Is

it conceivable that a simple deletion of the feedback receptor on the CSCs could allow for the delays and switching in cancer dynamics?

To test this hypothesis, we imposed a deletion of the feedback receptors in our CSC model. This deletion desensitizes CSCs to feedback entirely and immediately. We found, in agreement with the previous results reported in [20], that cancer growth initiated immediately and it was unrestricted (not shown). Even partial inhibition could not induce delays to CSC invasion [20]. Partial inhibition of the receptor does, however, limit the size of CSCs population, though this limit could be much larger than the healthy population.

Thus, mutations that simply remove sensitivity to the feedback signal cannot explain delayed onset to debilitating symptoms. We should note that a model of oncogenesis that requires a sequence of multiple mutations can potentially provide dynamics that is similar to our feedback model. In such multiple mutation model, delays can be introduced by the waiting times between successive mutations and the strong switch to the crisis phase might be induced by the final mutation which deletes the feedback receptor of the CSCs. Such model, however, offers no explanation as to origin of these delays between mutations nor can it predict the time of the onset of crisis phase, as we have done for our feedback interference model, eqn. (4).

Heterogeneity and Stochastic Dynamics May Lead to Cancer Extinction

One of the largest hurdles to overcome in understanding the genesis and progression of cancer is heterogeneity [31]. The characteristics of cancer vary wildly across different types of cancer, different patients, and ultimately different outcomes of many largely stochastic processes underlying cell population dynamics [32–34]. In the latter case, the progression of cancer can change due solely to chance. In other words two patients with precisely the same expected outcome (or two model simulations with the same parameters) may result in wildly different scenarios. We focus on this source of heterogeneity by simulating our model using a stochastic implementation (see detailed description in Methods).

The feedback interference mechanism that we propose is particularly sensitive to stochastic variation in cell division events. Feedback interference requires the interaction of two connected feedback loops (normal homeostatic feedback and feedback interference). Further, as we discuss above, the time of onset of the crisis phase depends critically on a small initial CSC population. Stochastic variation can have serious consequences when cell populations are small or involved in multiple feedbacks. Therefore, below, we implemented the same model described by equations (1–3) using the Gillespie method [25,26]. In the stochastic version of the model, each event (e.g. cell division) is given a probability to occur in the next small time step based on the right hand side of equations (1–3) and a draw of random numbers determines which event occurs. This is in contrast to the deterministic ODEs, where small changes in each cell count are calculated for every time step (see Methods for details).

We found qualitatively similar results between the stochastic and deterministic versions of the model. Both showed a delay from onset to crisis phase caused by a slow build up of *FI* which induced a release from feedback inhibition (Fig 3A,B). However, as predicted in the

discussion above, stochastic dynamics had a large impact, quantitatively, on the precise time of transition to crisis phase, T_{crisis} . Deterministic simulations (Fig 3A, black dashed line) produce drastically different T_{crisis} than the mean of all stochastic trials (Fig 3C, black dashed line). Further, the stochastic version of the model also led to high variability in T_{crisis} across individual trials (see Fig 3C).

One of the most interesting outcomes of the stochastic version of the model is that extinction of the CSC population is possible, even probable. Fig 3C shows CSC dynamics in different trials, some of which entered crisis phase at various times and grow rapidly. However, others (in fact the majority) underwent stochastically driven extinction (depicted in Figure 3C where CSC counts go to 0). Thus, a simulation with a unique set of parameters (or a patient) might have wildly different outcomes (extinction of CSCs or entrance to crisis phase) depending only on chance. It is worth noting that this scenario is not possible in the deterministic variant of the model. Multiple factors combine to yield a probable extinction in the stochastic model. First, all simulations here began with a small initial population of CSCs, thus, as each symmetric differentiation reduces the number of CSCs by one, this population of CSCs begins at risk for extinction. Second, at low levels of FI the feedback from DCs is largely intact, therefore the CSC population is nearly at equilibrium. But we saw previously (Fig 2D) that this means that symmetric proliferation and symmetric differentiation events happen nearly at the same rates. Therefore, in more than half of the stochastic trials tested, it was more probable to undergo enough symmetric differentiation events to deplete the small CSC population than it was to undergo enough symmetric proliferation events to build up FI and to escape a feedback control.

In the stochastic version of the model, even a single set of parameters can result in either extinction or transition to the crisis phase. Further, given that the system undergoes a specific transition (crisis or extinction), the time at which this happens varies wildly (Fig. 3D). We found that the distribution of T_{crisis} is roughly log-normal across all parameters. The coefficient of variation, the ratio of the standard deviation to the mean, was around 0.4 for all parameters, indicating high variability. Like the deterministic system, we found that the mean time to blast crisis increased as a function of $\frac{\beta\gamma_{cm}}{\alpha CSC_0}$, as in eqn. (4), see Fig. 3D, shown with increasing γ_{cm} . The probability of extinction also increased as a function of these parameters (Fig. 3E). Indeed for higher values of $\frac{\beta\gamma_{cm}}{\alpha CSC_0}$, would require a greater amount of FI to accumulate before making significant impact to block a feedback inhibition. This would give potentially more time for stochastic processes to lead to CSC population extinction.

The similarities between the deterministic and stochastic variants of the model are qualitative, both undergo a delay to crisis phase which increases with $\frac{\beta\gamma_{cm}}{\alpha CSC_0}$, but not quantitative. We found that in those cases where the stochastic system does not go extinct, it will undergo the transition to the crisis phase earlier than deterministic system (see Fig 3F). The T_{crisis} times for the stochastic variant of the model are based upon the condition that the

cancerous system, initiating with a single CSC, survived extinction (see Fig 3C). In order to survive extinction, the transition to crisis phase must occur before extinction. Effectively, extinction acted as a filter that removes trials that undergo this transition too late, and thus the remaining trials have a decreased T_{crisis} . From a dynamical systems point of view, the cancerous system starts close to the equilibrium point ($CSC = 0, FI = 0$), of a fast-slow system. The deterministic variant of the model first flows quickly onto the center manifold and then slowly away from the equilibrium point. Along the center manifold the speed increases non-linearly with distance from the equilibrium point. A small amount of stochastic variation can drastically accelerate the slow departure from the equilibrium point by pushing the cancer system further along the center manifold and hastening the transition to the crisis phase.

Our study predicts that heterogeneous effects, modeled here by different realizations of stochastic events, can lead to drastically different outcomes of cancer cell population dynamics: extinction of the CSC population or acceleration to crisis phase. Further, the fact that we observed that *most* trials lead to extinction before the crisis phase onset increases the burden of feedback escape that must be overcome by cancer. This provides a potential novel interpretation of cytostatic neoplasms as cancers whose CSC population went extinct before overcoming feedback escape. These issues reinforce the importance of examining cancerous systems in a stochastic context.

Targeted FI and CSC Treatments Make Profound Improvements over Chemotherapy

The mechanism of feedback interference that we describe above exposes a novel axis for treatment of cancer. Blocking the feedback interference signal should have a drastic impact on cancer systems mediated by feedback interference. We evaluated the possibility for a FI targeted treatment and compared its efficacy to current therapeutic approaches.

Chemotherapy is currently one of the primary approaches for treatment of cancer. It nonspecifically induces the death of cells that are replicating rapidly and thus it is very effective at debulking tumor size, but leaves patients prone to relapse. According to cancer stem cell theory [35,36], chemotherapy can affect only CDCs and not CSCs, leaving the CSCs able to regenerate the tumor. Recently, CSC-specific treatments have been identified and proposed in some types of cancer [9,23]. CSC targeted treatments have little effect on tumor size but selectively kill the CSCs that can affect relapse. However, CSC specific treatments are still in the early stages and limited to only a few types of cancer [9,23] and other modes of inhibiting CSC propagation are needed.

To implement treatment into our model we manipulated model parameters that were specific to the treatment type during the treatment period (Fig. 4). We calculated the reduction in tumor bulk and overall survival. Here, we defined a death event to occur when the tumor bulk ($CSCs$ and $CDCs$) exceed a given threshold (see Fig. 4A). Chemotherapy was implemented by imposing death of the CDC population (Fig. 4B inset). Despite the fact that this had no impact on CSCs (tumor generating cells), chemotherapy still reduced tumor bulk and therefore staved off transition to crisis phase so as to allow a greater chance of stochastically driven extinction (Fig. 4B). CSC-specific therapy was implemented by directly reducing the symmetric proliferation rate (Fig. 4C inset). This killed the tumor

generating *CSCs*, but left the *CDC* population, which represent the majority of the tumor, intact (Fig. 4C). Finally, our novel *FI*-directed treatment was implemented by increasing the death rate of *FI* (Fig. 4D). This stopped the growth of tumor generating *CSCs* by keeping them in control of normal homeostatic feedbacks. This did not directly kill the *CSC* population but did keep the *CSC* growth rate very low and allowed stochastically driven extinction to eventually eradicate this small *CSC* population. Our *FI*-directed treatment also left the *CDC* population intact.

To compare the efficacy of different treatment strategies we ran multiple stochastic trials and quantified the results using the “survival rate”. The transition to crisis phase, defined here as the tumor bulk exceeding a certain threshold (see Fig. 4), was classified as a “lethal event”. Survival was quantified as the number of stochastic trials that remained in chronic phase (Fig 4E–F). Larger fraction of such trials would constitute better survival rate in our model.

Despite debulking large portions of the tumor, chemotherapy made only slight improvements on average over scenarios without treatment (Fig. 4E). In the model that we present here, the tumor is generated by the *CSCs* which are untouched by chemotherapy. Thus, even tumors with greatly reduced *CDC* population (as a result of chemotherapy) can regenerate the tumor and enter crisis phase solely due to overgrowth of *CSCs*. Chemotherapy, however did show slight improvements over scenarios without treatment. Loss of *CDCs*, due to chemotherapy, effectively delays the time at which the tumors could reach the threshold bulk amount for a lethal event. This delay prolonged the time in the chronic phase where *CSC* counts are low and susceptible to stochastically driven extinction.

The model of *CSC* targeted therapy was very effective. In almost every implementation, we found a 100% survival rate (Fig. 4E–F). *CSC*-targeted treatment destroys the tumor generating *CSCs* and thus leaves tumor cytostatic. It should be noted that the majority of the tumor (the population of *CDCs*) remains even after treatment, but cannot grow or progress the disease to the crisis phase.

The novel *FI*-directed treatment was not as successful as the *CSC*-specific treatment but still revealed large improvements in survival rate (Fig. 4E–F). We found that *FI*-targeted therapy was effective at controlling the growth-rate of the *CSC* population. While it did not kill *CSCs* directly, it kept growth rate low and allowed stochastically driven extinction to eradicate the *CSC* population. This mechanism, also revealed a strong dependence of treatment success on the treatment duration (Fig. 4G). Long durations of *FI*-treatment had stronger effects on the *CSC* population.

The feedback interference mechanism for cancer progression is strongly dependent on the feedback interference signal, *FI*. This provides a novel axis for cancer treatment. We showed while this is not as effective as *CSC*-targeted therapy, it still can have profound effects on survival rate and outperforms chemotherapy in *CSC*-dependent cancers. *FI*-targeted therapy could provide an attractive option, especially in cases where *CSC*-targeted therapy was not available.

Discussion

Long delays are known to exist in the progression of many types of cancer where initial cancerous populations remain small until a sudden shift to an aggressive crisis phase [1,2]. These delays offer the opportunity for early intervention and better patient prognosis. However, the mechanisms that confer these delays or induce the shift from asymptomatic to crisis phases are still unknown. In this study, we proposed a dynamic model of healthy and cancerous cell populations to explain the delay between the time of carcinogenic genetic mutations and the onset of clinical symptoms in stem cell cancers, such as leukemia. Our model describes a mechanism where an extracellular factor, *FI*, produced by cancerous stem cells progressively disrupts the normal homeostatic feedback from differentiated cell types to stem cells. This leads to a strong and sudden shift in growth rate of cancer cells preceded by a long dormancy period, where cancerous cell populations are kept low, as was observed in clinical studies [1].

Feedback is critical in order to maintain homeostasis. Our model predicts, as have others [20], that feedback from differentiated cell populations imposes a single stable homeostatic state where both stem and differentiated cells are maintained. This stability is critical during injury, where loss of differentiated cell population invokes the stem cell system to return to the appropriate amounts of stem and differentiated cells. Candidate feedback signals have been found in many stem cell systems. For example, in the stem cell regulation of the olfactory epithelium, GDF11 is secreted by differentiated neurons and controls the actions of progenitors [16]. The regulation of blood production, which is critical for diseases like CML, involves many different feedback signals (e.g. VEGF, TGF- β) that regulate the actions of upstream stem cells and progenitors [14]. Indeed, many cancers show mutations in these critical feedback pathways. The Wnt pathway, critical in regulating hematopoiesis [37–39], is also mutated in many different cancers [18,24,40].

The feedback interference mechanism of cancer initiation, proposed in our study, specifically disrupts these normal feedback signals in a dose-dependent manner. This dependency on the amount of *FI*, critical for the delay mechanism discussed, can be characterized as a modification of the microenvironment by the CSCs that establishes a niche for cancer progression. Like healthy cells, the physical [6] and biochemical [7] microenvironment is critical in determining cancer cell fate and function. It is known that cancer, and in particular CSCs, modify their local microenvironment to achieve this goal [7]. In many cases this is done by secreting extracellular signaling molecules. For example, in glioblastoma-multiformae CSCs are known to secrete VEGF, an angiogenesis factor, [8]; in pancreatic cancer CSCs secrete the TGF- β signal Nodal and its receptor, which increased self renewal capacity [9]; in colon cancer CSCs secrete HGF, acting through Wnt, to keep CSCs in an undifferentiated state [10]. Thus, CSCs modify their local environment via secretory signals, and, in some cases [9,10], these signals specifically alter the stem cell differentiation program as proposed in our model. This leads to increased stem cell proliferation and, eventually, transition to crisis phase, in agreement with our model predictions.

Tumors have a large impact on their microenvironment through the signals they secrete and the invasive actions they take (e.g. degradation of the extra-cellular matrix). This interplay between the local environment and cancer strongly affects the rate of tumor progression. The relative role of environmental and genetic influences of cancer progression remains an active area of research. To investigate whether mutations could induce delay in our model we imposed a genetic deletion of a feedback receptor on the CSCs. This initiated immediate transition into crisis phase and therefore cannot account for the delays seen in cancers like CML, pancreatic, and colorectal cancer [1,2]. In contrast, our feedback interference model produced a delay that depended on the initial *CSC* count, the amount of *FI* produced by *CSCs*, and effectiveness of the *FI* impact on the normal feedback inhibitory mechanisms. It should be noted that many of the cancers do acquire multiple different mutations before progression into crisis phase [3], and the connection between genetic and environmental influences on the progression of cancer is still active area of research.

Genomic studies of cancer show that the disease presents with many different sources of heterogeneity: between cell or cancer types, between patients, and (among others) within subpopulations of the tumor itself [41,42]. To explore the role of heterogeneity of cancers and the variance in patient outcomes, we implemented a stochastic model of cancer cell population dynamics. Individual trials represent different outcomes of the stochastic processes that initiate cancer. We found, as have others [20], that the cancer stem cell population can go extinct due to purely stochastic effects. Starting from a small amount of cancerous stem cells, a small number of symmetric differentiation events will extinguish the population. This indicates that the initial portion of chronic phase is a critical period deciding between one two divergent outcomes: stochastic extinction of *CSCs* or transition to crisis phase. During this critical period treatment efforts may be most effective as the *CSC* population may only require encouragement to undergo stochastically driven extinction. This type of extinction may also offer insight into the inability for some early stage tumors to transition to more aggressive stages, for example in colorectal cancer [3], or the existence of non-expansive benign tumors.

The identification of a novel mechanism for delay between chronic and critical phases in cancer progression provides an opportunity for a novel approach to therapy. In the feedback interference mechanism we propose the interference is mediated by a chemical signal, *FI*, which could be a potential drug target. While *FI*-targeted treatment did not have the same impact of *CSC*-targeted treatments, our model predicted that it does significantly increase survival. The novel *FI*-targeted treatment may not be ideal in scenarios where options such as *CSC*-targeted treatment are available. However, *FI*-targeted therapy may offer an effective alternative that can delay the progression of cancer long enough so as stochastically driven extinction of the *CSC* population may occur.

Conclusions

Homeostatic feedback is critical for stem cell regulation. We propose that interference in this circuit can promote cancerous conditions. This mechanism of cancer initiation replicates the biphasic nature of certain chronic cancers, such as CML, pancreatic, and colorectal cancer where long delays exist between largely asymptomatic and lethal phases. These delays may

not be restricted to chronic cancers. Standard treatment options, such as chemotherapy, can extend delays between treatment and relapse. However, novel treatment options targeting cancer stem cell population have the potential to decrease or eliminate relapse. Some of these treatments have already been explored in animal model systems leading to cancer reduction [23]. Further experimental and modeling studies are needed to test these predictions.

Supplementary Material

Refer to Web version on PubMed Central for supplementary material.

References

1. Lee SJ. Chronic myelogenous leukaemia. *Br J Haematol*. 2000; 111:993–1009. [PubMed: 11167734]
2. Yachida S, Jones S, Bozic I, Antal T, Leary R, Fu B, et al. Distant metastasis occurs late during the genetic evolution of pancreatic cancer. *Nature*. 2010; 467:1114–1117. [PubMed: 20981102]
3. Fearon ER, Vogelstein B. A genetic model for colorectal tumorigenesis. *Cell*. 1990; 61:759–767. [PubMed: 2188735]
4. Radich JP, Dai H, Mao M, Oehler V, Schelter J, Druker B, et al. Gene expression changes associated with progression and response in chronic myeloid leukemia. *Proc Natl Acad Sci U S A*. 2006; 103:2794–2799. [PubMed: 16477019]
5. McCormack PL, Keam SJ. Dasatinib. *Drugs*. 2012; 71:1771–1795. DOI: 10.2165/11207580-000000000-00000
6. Bissell MJ, Hall HG, Parry G. How does the extracellular matrix direct gene expression? *J Theor Biol*. 1982; 99:31–68. [PubMed: 6892044]
7. Paltridge JL, Belle L, Khew-Goodall Y. The secretome in cancer progression. *Biochim Biophys Acta BBA-Proteins Proteomics*. 2013; 1834:2233–2241. [PubMed: 23542208]
8. Bao S, Wu Q, McLendon RE, Hao Y, Shi Q, Hjelmeland AB, et al. Glioma stem cells promote radioresistance by preferential activation of the DNA damage response. *Nature*. 2006; 444:756–760. DOI: 10.1038/nature05236 [PubMed: 17051156]
9. Lonardo E, Hermann PC, Mueller M-T, Huber S, Balic A, Miranda-Lorenzo I, et al. Nodal/Activin signaling drives self-renewal and tumorigenicity of pancreatic cancer stem cells and provides a target for combined drug therapy. *Cell Stem Cell*. 2011; 9:433–446. [PubMed: 22056140]
10. Vermeulen L, Felipe De Sousa EM, van der Heijden M, Cameron K, de Jong JH, Borovski T, et al. Wnt activity defines colon cancer stem cells and is regulated by the microenvironment. *Nat Cell Biol*. 2010; 12:468–476. [PubMed: 20418870]
11. Jamieson CH. Chronic Myeloid Leukemia Stem Cells. *ASH Educ Program Book*. 2008; 2008:436–442. DOI: 10.1182/asheducation-2008.1.436
12. O'Brien CA, Pollett A, Gallinger S, Dick JE. A human colon cancer cell capable of initiating tumour growth in immunodeficient mice. *Nature*. 2007; 445:106–110. DOI: 10.1038/nature05372 [PubMed: 17122772]
13. Komarova NL. Principles of Regulation of Self-Renewing Cell Lineages. *PLOS ONE*. 2013; 8:e72847.doi: 10.1371/journal.pone.0072847 [PubMed: 24019882]
14. Kirouac DC, Ito C, Csaszar E, Roch A, Yu M, Sykes EA, et al. Dynamic interaction networks in a hierarchically organized tissue. *Mol Syst Biol*. 2010; 6 Available: <http://msb.embopress.org/content/6/1/417.abstract>.
15. Lander AD, Gokoffski KK, Wan FY, Nie Q, Calof AL. Cell lineages and the logic of proliferative control. *PLoS Biol*. 2009; 7:e1000015.
16. Wu H-H, Ivkovic S, Murray RC, Jaramillo S, Lyons KM, Johnson JE, et al. Autoregulation of neurogenesis by GDF11. *Neuron*. 2003; 37:197–207. [PubMed: 12546816]

17. McPherron AC, Lawler AM, Lee S-J. Regulation of skeletal muscle mass in mice by a new TGF-p superfamily member. *Nature*. 1997; 387:83–90. DOI: 10.1038/387083a0 [PubMed: 9139826]
18. Lento W, Congdon K, Voermans C, Kritzik M, Reya T. Wnt signaling in normal and malignant hematopoiesis. *Cold Spring Harb Perspect Biol*. 2013; 5:a008011. [PubMed: 23378582]
19. Khalek FJA, Gallicano GI, Mishra L. Colon cancer stem cells. *Gastrointest Cancer Res GCR*. 2010:S16. [PubMed: 21472043]
20. Rodriguez-Brenes IA, Komarova NL, Wodarz D. Evolutionary dynamics of feedback escape and the development of stem-cell–driven cancers. *Proc Natl Acad Sci*. 2011; 108:18983–18988. [PubMed: 22084071]
21. Barker N, Ridgway RA, van Es JH, van de Wetering M, Begthel H, van den Born M, et al. Crypt stem cells as the cells-of-origin of intestinal cancer. *Nature*. 2009; 457:608–611. DOI: 10.1038/nature07602 [PubMed: 19092804]
22. Orkin SH, Zon LI. Hematopoiesis: An Evolving Paradigm for Stem Cell Biology. *Cell*. 2008; 132:631–644. DOI: 10.1016/j.cell.2008.01.025 [PubMed: 18295580]
23. Liu X, Johnson S, Liu S, Kanojia D, Yue W, Singh UP, et al. Nonlinear Growth Kinetics of Breast Cancer Stem Cells: Implications for Cancer Stem Cell Targeted Therapy. *Sci Rep*. 2013; 3 Available: http://www.nature.com/srep/2013/130820/srep02473/full/srep02473.html?WT.ec_id=SREP-631-20130902.
24. Jamieson CH, Ailles LE, Dylla SJ, Muijtjens M, Jones C, Zehnder JL, et al. Granulocyte–macrophage progenitors as candidate leukemic stem cells in blast-crisis CML. *N Engl J Med*. 2004; 351:657–667. [PubMed: 15306667]
25. Gillespie DT. A general method for numerically simulating the stochastic time evolution of coupled chemical reactions. *J Comput Phys*. 1976; 22:403–434.
26. Gillespie DT. Exact stochastic simulation of coupled chemical reactions. *J Phys Chem*. 1977; 81:2340–2361. DOI: 10.1021/j100540a008
27. Xiong W, Ferrell JE. A positive-feedback-based bistable “memory module” that governs a cell fate decision. *Nature*. 2003; 426:460–465. DOI: 10.1038/nature02089 [PubMed: 14647386]
28. Sneppen K, Micheelsen MA, Dodd IB. Ultrasensitive gene regulation by positive feedback loops in nucleosome modification. *Mol Syst Biol*. 2008; 4:182.doi: 10.1038/msb.2008.21 [PubMed: 18414483]
29. Brandman O, Meyer T. Feedback loops shape cellular signals in space and time. *Science*. 2008; 322:390–395. DOI: 10.1126/science.1160617 [PubMed: 18927383]
30. Freeman M. Feedback control of intercellular signalling in development. *Nature*. 2000; 408:313–319. DOI: 10.1038/35042500 [PubMed: 11099031]
31. Burrell RA, McGranahan N, Bartek J, Swanton C. The causes and consequences of genetic heterogeneity in cancer evolution. *Nature*. 2013; 501:338–345. DOI: 10.1038/nature12625 [PubMed: 24048066]
32. Gupta PB, Fillmore CM, Jiang G, Shapira SD, Tao K, Kuperwasser C, et al. Stochastic State Transitions Give Rise to Phenotypic Equilibrium in Populations of Cancer Cells. *Cell*. 2011; 146:633–644. DOI: 10.1016/j.cell.2011.07.026 [PubMed: 21854987]
33. Wilkinson DJ. Stochastic modelling for quantitative description of heterogeneous biological systems. *Nat Rev Genet*. 2009; 10:122–133. DOI: 10.1038/nrg2509 [PubMed: 19139763]
34. Lahav G, Rosenfeld N, Sigal A, Geva-Zatorsky N, Levine AJ, Elowitz MB, et al. Dynamics of the p53-Mdm2 feedback loop in individual cells. *Nat Genet*. 2004; 36:147–150. DOI: 10.1038/ng1293 [PubMed: 14730303]
35. Pardal R, Clarke MF, Morrison SJ. Applying the principles of stem-cell biology to cancer. *Nat Rev Cancer*. 2003; 3:895–902. DOI: 10.1038/nrc1232 [PubMed: 14737120]
36. Reya T, Morrison SJ, Clarke MF, Weissman IL. Stem cells, cancer, and cancer stem cells. *Nature*. 2001; 414:105–111. DOI: 10.1038/35102167 [PubMed: 11689955]
37. Austin TW, Solar GP, Ziegler FC, Liem L, Matthews W. A role for the Wnt gene family in hematopoiesis: expansion of multilineage progenitor cells. *Blood*. 1997; 89:3624–3635. [PubMed: 9160667]

38. Corrigan PM, Dobbin E, Freeburn RW, Wheadon H. Patterns of Wnt/Fzd/LRP gene expression during embryonic hematopoiesis. *Stem Cells Dev.* 2009; 18:759–772. DOI: 10.1089/scd.2008.0270 [PubMed: 18800919]
39. Reya T, Duncan AW, Ailles L, Domen J, Scherer DC, Willert K, et al. A role for Wnt signalling in self-renewal of haematopoietic stem cells. *Nature.* 2003; 423:409–414. [PubMed: 12717450]
40. Abrahamsson AE, Geron I, Gotlib J, Dao K-HT, Barroga CF, Newton IG, et al. Glycogen synthase kinase 3 β missplicing contributes to leukemia stem cell generation. *Proc Natl Acad Sci.* 2009; 106:3925–3929. [PubMed: 19237556]
41. Lawrence MS, Stojanov P, Polak P, Kryukov GV, Cibulskis K, Sivachenko A, et al. Mutational heterogeneity in cancer and the search for new cancer-associated genes. *Nature.* 2013; 499:214–218. [PubMed: 23770567]
42. Landau DA, Carter SL, Stojanov P, McKenna A, Stevenson K, Lawrence MS, et al. Evolution and impact of subclonal mutations in chronic lymphocytic leukemia. *Cell.* 2013; 152:714–726. [PubMed: 23415222]

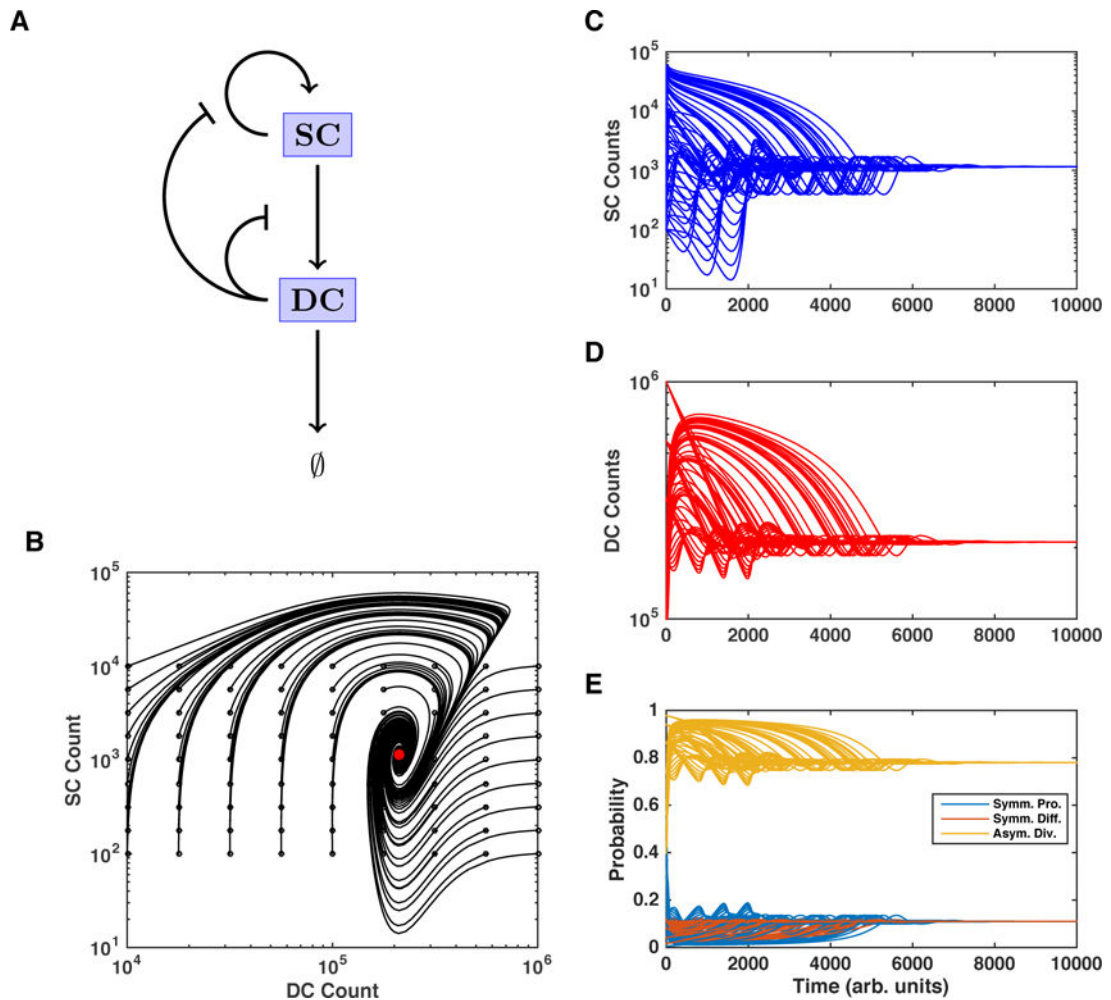


Fig 1. Normal Stem Cell Model Dynamics

A) Model of normal cell growth. Stem Cells are capable of proliferation and differentiation to DCs who eventually die. Feedback from DCs mediates the division rate and profile (see Methods). See supplement for parameters. B) Phase plot of SC and DC populations. Phase trajectories are shown for different initial conditions (black circles). All simulations end at the same equilibrium (red dot). C, D) Dynamics of SCs (C) and DCs (D) for different initial conditions. E) Probability profile of different division types. Equilibrium is reached when symmetric differentiation matches symmetric proliferation.

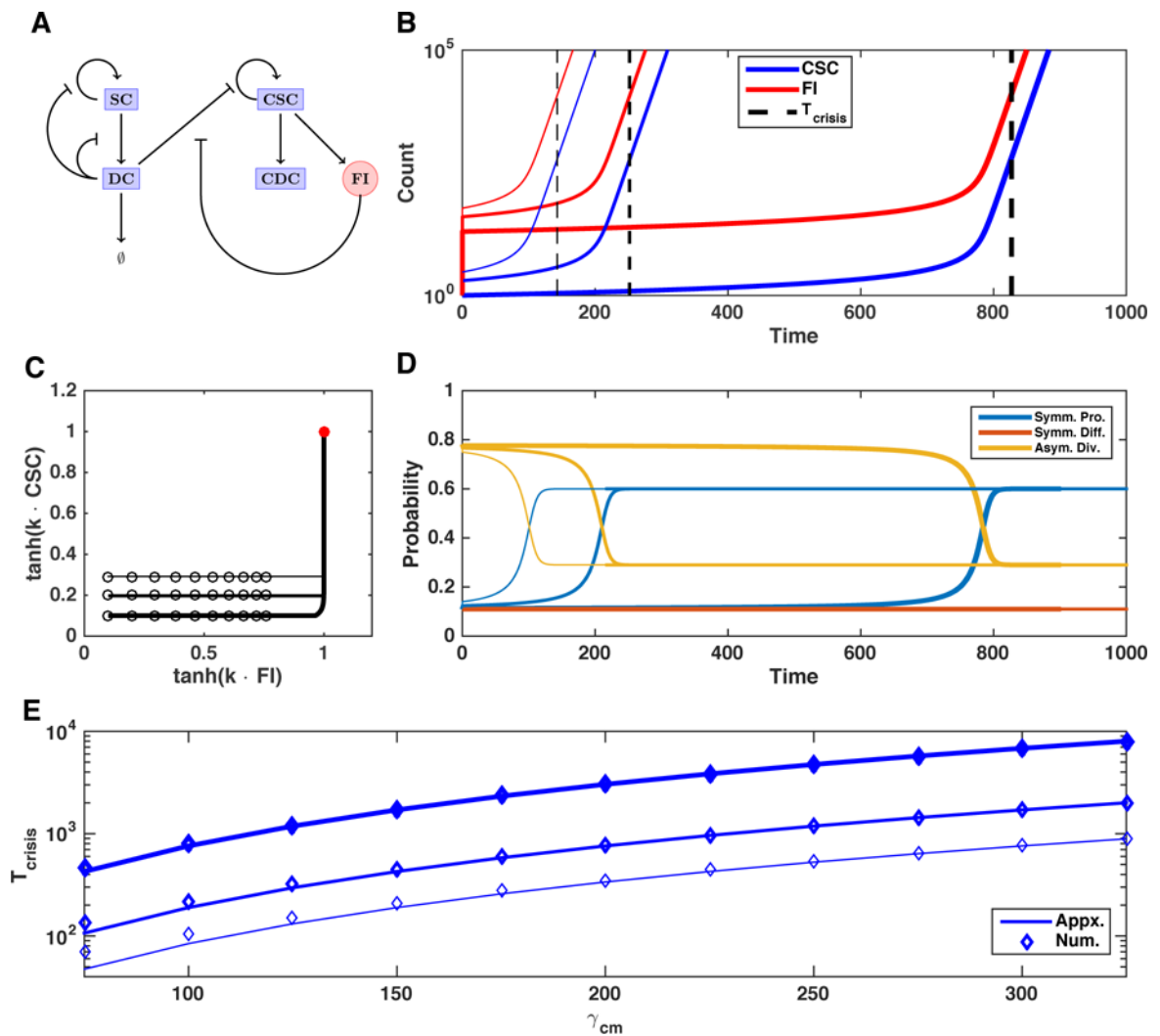


Fig 2. Cancer Stem Cell Dynamics

A) Model of cancer cell growth. Cancer Stem Cells create a feedback interference signal, FI , that disinhibits feedback from DCs to CSCs. B) Time course of the cancer system.

Trajectories corresponding to a single initial CSC are denoted by thick lines, whereas those for initial CSC count of two or three are progressively thinner lines. Dynamics of the cancer system starting from different initial conditions show a long period where tumor growth is slow followed by a sharp transition to fast growth. The black dashed line denotes the time which we defined as T_{crisis} .

C) Phase plot of the CSC and FI. Phase trajectories are shown for different initial conditions (black circles). Trajectories corresponding to a single initial CSC are denoted by thick lines, whereas those for initial CSC count of two or three are progressively thinner lines. Axes are in terms of a scaled hyperbolic tangent of the variables (here $k = 0.1$), thus, $\tanh(k \cdot CSC) \rightarrow 1$ as $CSC \rightarrow \infty$. Note, that trajectories all grow unboundedly in time (red dot).

D) Probability profile of division types shows a strong switch at T_{crisis} favoring symmetric proliferation. Trajectories for a single initial CSC are denoted by thick lines, whereas those for initial CSC count of two or three are progressively thinner lines.

E) Comparison of analytical estimate of T_{crisis} with numerically calculated value for

multiple combinations of feedback interference threshold, γ_{cm} and initial CSC count. Trajectories for a single initial CSC are denoted by thick lines, where as those for initial CSC count of two or three are progressively thinner lines.

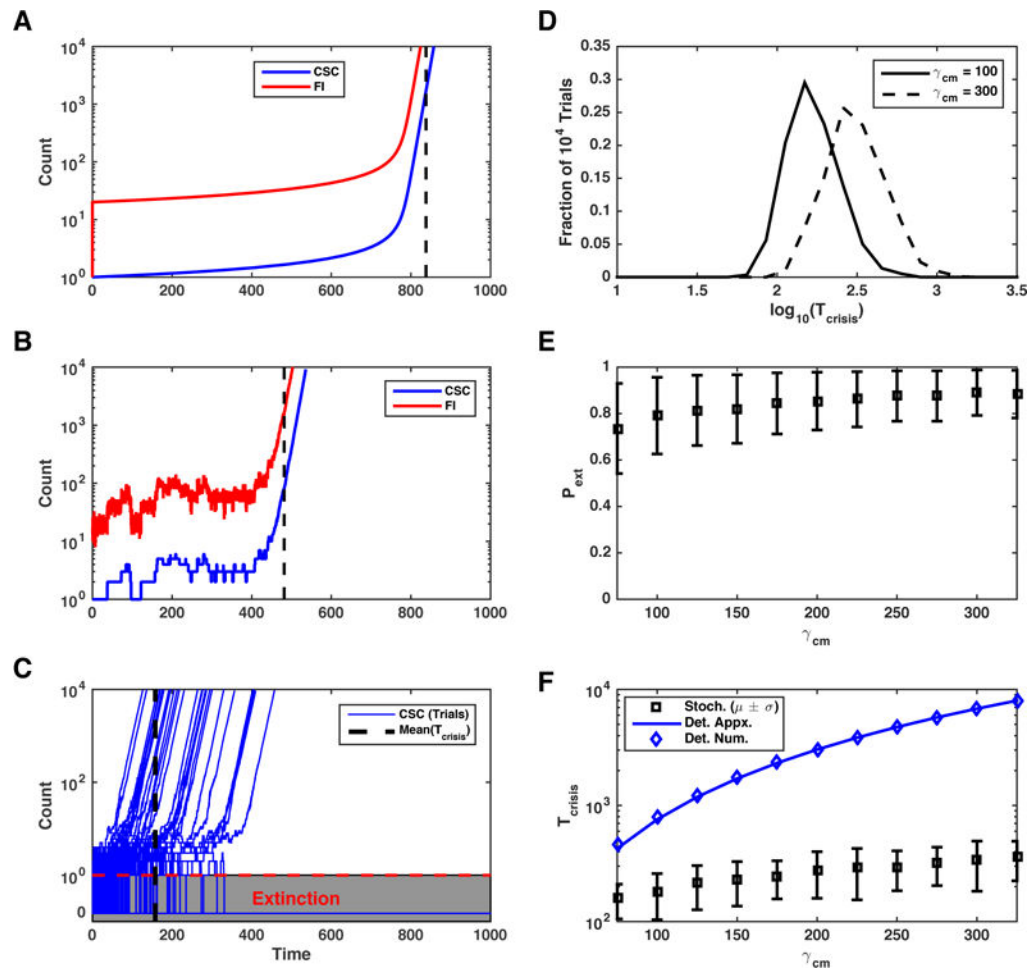


Fig 3. Heterogeneity via Stochastic Dynamics

A,B) Comparison of deterministic (A) and a single trial of a stochastic (B) simulation for the exact same parameters with a single initial CSC. Dashed lines represent calculated T_{crisis} . C) Many trials of stochastic simulation with the same parameters as in A) and B). Dashed black line denotes the mean over trials of calculated T_{crisis} . Plot is given in log plot above red dashed line, below this line we also show CSC=0 to show extinction. D) Distribution of $\log_{10}(T_{crisis})$ for two different values of γ_{cm} . E) Mean plus and minus one standard deviation of the Probability of extinction, P_{ext} for numeric stochastic simulations is plotted for various levels of the interference threshold, γ_{cm} . F) T_{crisis} is plotted in log-scale as calculated from the deterministic variant of the model analytically (blue curve) and numerically (blue diamonds). This is compared with the mean plus and minus standard deviation of T_{crisis} in the stochastic variant of the model.

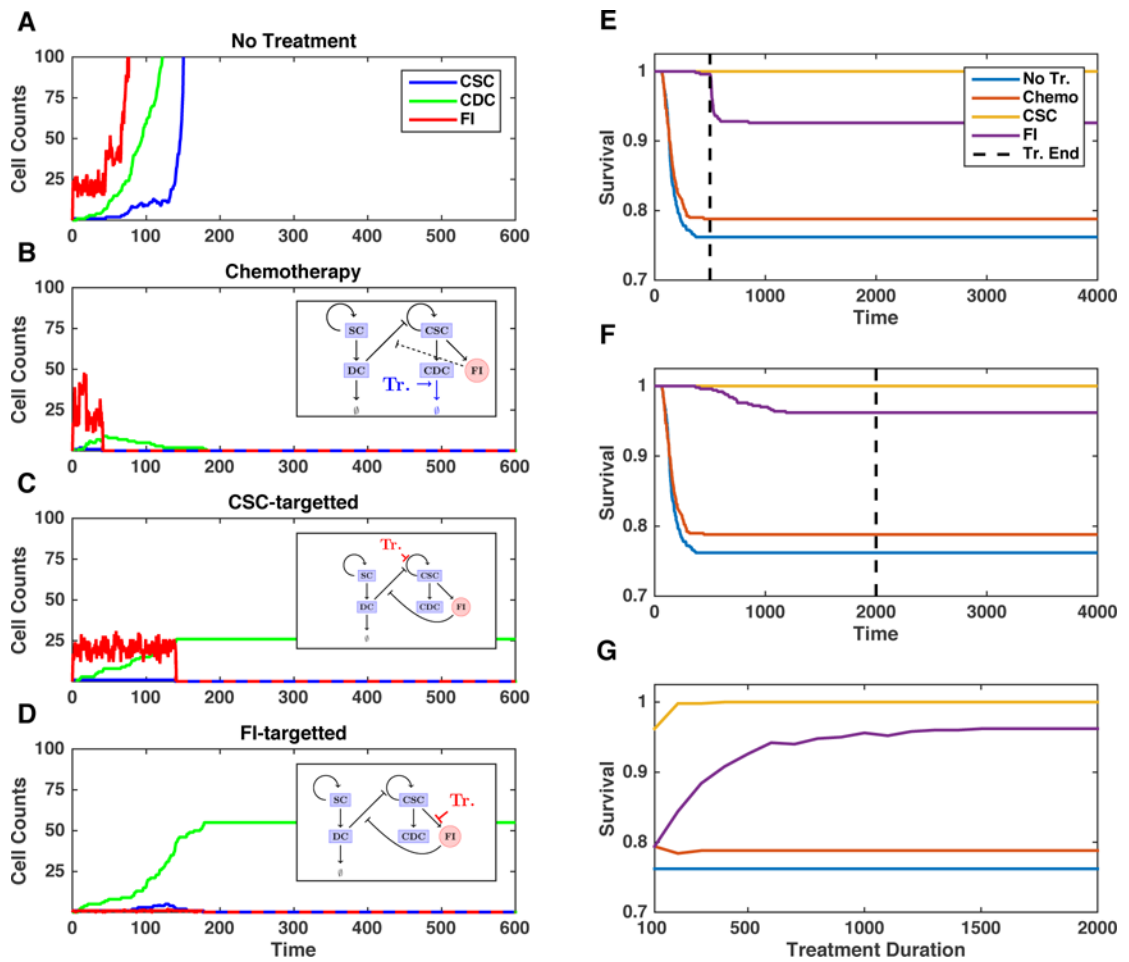


Figure 4. Efficacy of Treatment Strategies

A–D) Example trials of the cancer system dynamics where no treatment (A), chemotherapy (B), *CSC*-targetted therapy (C), or *FI*-targetted therapy is employed. In each case therapy is given for the entire duration shown. Stick models of the implementation of treatment are shown in the inset, see Methods for details. E–F) Survival rate under different treatment conditions (see colors) and durations (see black dashed line). G) Survival is given as a function of treatment duration.

Table 1

Summary of Events in Stochastic Version of the Model.

| Event | Propensity (Rate) | State Change |
|----------------------|---|---|
| Sym. Renewal of SCs | $p(DC)v(DC)SC$ | $SC \rightarrow SC + 1$ |
| Sym. Diff. of SCs | $q(DC)v(DC)SC$ | $SC \rightarrow SC - 1,$ $DC \rightarrow DC + 1$ |
| Asym. Diff. of SCs | $[1 - p(DC) - q(DC)]v(DC)SC$ | $DC \rightarrow DC + 1$ |
| DC Death | dDC | $DC \rightarrow DC - 1$ |
| Sym. Renewal of CSCs | $\bar{p}(DC, FI)v(DC)CSC$ | $CSC \rightarrow CSC + 1$ |
| Sym. Diff. of CSCs | $q(DC)v(DC)CSC$ | $CSC \rightarrow CSC - 1,$ $CDC \rightarrow CDC + 1$ |
| Asym. Diff. of CSCs | $[1 - \bar{p}(DC, FI) - q(DC)]v(DC)CSC$ | $CDC \rightarrow CDC + 1$ |
| Birth of FI | $\alpha.CSC$ | $FI \rightarrow FI + 1$ |
| Death of FI | βFI | $FI \rightarrow FI - 1$ |

Author Manuscript

Author Manuscript

Author Manuscript

Author Manuscript